Available online at www.sciencedirect.com
SCIENCE DIRECT®
Journal of the European Ceramic Society 26 (2006) 289–295
www.elsevier.com/locate/jeurceramsoc

Untypical Young's modulus evolution of model refractories at high temperature

N. Tessier-Doyen[a], J.C. Glandus[b], M. Huger[b,*]

[a] *Laboratoire "Mécanique, Matériaux et Procédés de Fabrication", 61 rue Albert Camus, 68093 Mulhouse Cedex, France*
[b] *GEMH, Ecole Nationale Supérieure de Céramique Industrielle, 47 à 73 avenue Albert Thomas, 87065 Limoges Cedex, France*

Received 10 July 2004; received in revised form 27 October 2004; accepted 29 October 2004
Available online 5 January 2005

Abstract

Industrial refractories can exhibit untypical Young's modulus behaviour versus temperature, characterized by hysteretic loops in the plot $E_{(T)}$. This paper shows how the use of simplified model materials helps in the understanding of such behaviours, obviously depending both on the properties of each component of the refractory material and on the presence of internal defects. Model materials constituted of a hot-pressed glass matrix surrounding spherical alumina inclusions have been studied. Glasses exhibiting various coefficients of thermal expansion (CTE) have been used as matrix in order to obtain three typical microstructural configurations ($\Delta\alpha < 0$, $\Delta\alpha = 0$ and $\Delta\alpha > 0$, where $\Delta\alpha$ denotes the CTE difference between matrix and inclusions).

Keywords: Refractories; Thermal expansion; Young's modulus; Al_2O_3/glass

1. Introduction

Industrial refractories are multiphased materials with extremely wide chemical composition in terms of binding phase, aggregates and organic additives. So, they exhibit generally complex heterogeneous microstructures which can give rise to high internal thermal stresses. Because of volume expansion mismatch or phase changes, the service conditions can greatly affect their initial microstructural state so as their thermomechanical properties.

The purpose of this paper is to investigate the effect of thermal expansion mismatch on elastic properties of debonded and microcracked materials. Temperature variations can lead either to interfacial separation between aggregates and matrix or to microcracks, both depending on the range of CTE mismatch between the components. Such effects modify all the material thermomechanical properties, specially Young's modulus, strongly dependent on microstructure and composition.

Firstly, typical Young's modulus temperature dependencies will be presented: this of industrial refractories of the alumina/carbon family then those of three model materials for which the chemical nature of aggregates remain the same. Finally, E values calculated using an analytical model will be compared to experimental results.

2. Example of untypical high temperature Young's modulus evolution of industrial refractories

2.1. Elastic modulus measurement

Young's modulus measurement during a thermal cycle was carried out using an ultrasonic technique described elsewhere.[1] A wideband pulse of ultrasonic compressional wave is obtained by subjecting a magnetostrictive material to a magnetic field. The ultrasonic wave propagation through the studied materials is ensured by an alumina wave guide attached to the sample by a refractory cement.

* Corresponding author. Tel.: +33 5 5545 2222; fax: +33 5 5579 0998.
E-mail address: m_huger@ensci.fr (M. Huger).

0955-2219/$ – see front matter © 2004 Elsevier Ltd. All rights reserved.
doi:10.1016/j.jeurceramsoc.2004.10.028

The Young's modulus, E, is calculated using the well-known relationship:

$$E = \rho\left(\frac{2L}{\tau}\right)^2$$

in which τ is the time delay between two successive echoes corresponding to a round-trip within the sample, L the sample length and ρ is the material density. The great sensitivity of waves velocity to the material microstructure leads to calculated E effects which can be considered as pertinent behaviour indicators of multiphased materials at high temperature.

2.2. Alumina/carbon-shaped refractories

Ladle shrouds are components used in continuous steel casting to protect metal against oxidation. At the beginning of the process, these cylindrical parts (several tens of millimetre in thickness) are usually at room temperature when the molten steel, at temperature up to 1550 °C, suddenly flows inside. Al_2O_3/C refractories similar to those used for ladle shrouds have been studied.[2] They are composed of Al_2O_3 coarse grains and graphite flakes in a matrix bonded by a phenolic resin. Anti-oxidant compounds are added. After isostatic pressing, materials are fired at 1000 °C in inert atmosphere. Then, after firing, the material cohesion is ensured by the pyrocarbon resulting from the phenolic resin pyrolysis. When they are subjected to heating/cooling cycles, their Young's modulus exhibits hysteresis effects.

Fig. 1 shows results obtained for a 62 vol.% alumina composition sample during temperature cycles performed at 5 °C min^{-1} between 20 and 850 °C. It can be noticed the very low Young's modulus initial value, well suited to ladle shroud applications (specially thermal shocks[3]). Contrary to stable fine ceramics which exhibit regular reversible E decrease when the temperature increases, strong nonlinear and irreversible effects are observed. The large increase from 450 to 650 °C can be attributed to the closure of interparticle decohesions and cracks due to the thermal expansion mismatch. Regarding the CTE difference between the alumina grains and the carbon matrix, the presence of decohesions surrounding alumina grains seems to be responsible for this specific behaviour. When cooling, under 650 °C, the Young's modulus decrease is due to decohesions and cracks opening.

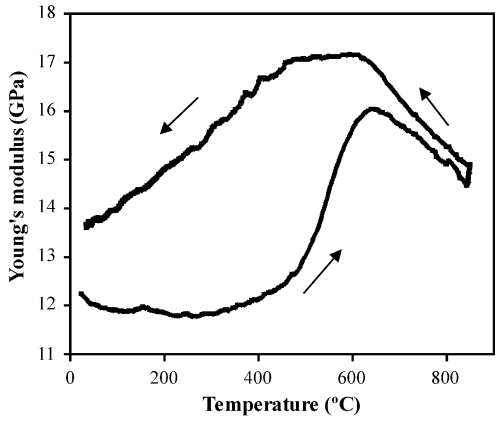

Fig. 1. Evolution of the Young's modulus of an alumina/carbon refractory with temperature.

3. Model materials as predicting tools

3.1. Description of the approach

Such non-conventional behaviours are not easy to describe accurately because a lot of mechanisms, which can occur simultaneously, arise during the heating/cooling cycles. So, the influence of discontinuous interfaces and cracks is experimentally observable but remains difficult to analyse.

Obviously, macroscopic Young's modulus phenomena are closely linked to the temperature behaviour of each constituent of the refractory material. But these constituents are generally numerous and their individual influences cannot be characterized easily.

The most convenient approach consists to reduce the microstructure to two constituents only. Indeed, it allows the study of biphased model materials exhibiting simplified behaviours. Depending both on the sign of the CTE mismatch between the two phases ($\Delta\alpha = \alpha_m - \alpha_p$) and on the microstructure, various phenomena can occur when a sample is cooled to room temperature (interfacial debonding, microcracking or adjusted interfaces).

The studied biphased samples contain randomly dispersed alumina particles whose physical and chemical characteristics are close to those of the aggregates used in industrial refractories previously presented. The binding phase is chosen in order to obtain an isotropic, homogeneous and inert material whose thermal expansion coefficient is adjustable to this of inclusions. So, glasses were chosen because their coefficient of thermal expansion is easily adjustable by modifying the oxides proportions in their chemical composition.

3.2. Young's modulus at room temperature

3.2.1. Model material preparation and characterization

Glass/alumina particles specimens are prepared using three different borosilicate glasses as matrix, which are referenced G1, G2 and G3 by growing CTE (Table 1). The dispersed phase is constituted of 99.9% pure alumina balls. For each biphased system, three controlled volume fractions of inclusions (15, 30 and 45%) were added to fine glass powder. Organic additives are used to facilitate the shaping by cold uni-axial pressing of the mixture. After a binding removal treatment, a post-hot-pressing stage (p = 15 MPa, $T = T_g + 200$ °C) in a wolfram carbide die is performed in order to reduce the matrix porosity. Then specimens are naturally cooled to room temperature with a cooling rate of about 10 °C min^{-1}.

Table 1
Thermoelastic properties of the constituents

	Designation	E (GPa)	Poisson's ratio (ν)	α[a] ($10^{-6}\,K^{-1}$)	$\Delta\alpha$ ($10^{-6}\,K^{-1}$)	T_g (°C)
Dispersed particles						
α-Alumina (99.9%)	Spherical (500 μm)	340	0.24	7.6	–	–
Glass matrix						
Amorphous	G1	68	0.20	4.6	−3.0	595
Amorphous	G2	76	0.21	7.4	−0.2	605
Amorphous	G3	72	0.23	11.6	4.0	470

[a] Measured by dilatometric technique between 50 and 450 °C.

The Fig. 2 shows micrographs of polished surfaces of alumina/G1 and alumina/G3 specimens containing 15 vol.% of inclusions. The particles shape is not perfectly spherical and the alumina/G1 system ($\alpha_m < \alpha_p$) shows a dark interfacial zone which can be due to a gap arising during cooling (Fig. 2a). For alumina/G3 system which exhibits greater CTE matrix, cracks in the matrix and around alumina inclusions can be optically observed using a fluorescent UV dye penetrant (Fig. 2b). Neither matrix cracks nor interfacial debonding are observed for alumina/G2 samples ($\alpha_m \approx \alpha_p$).

The samples porosity is derived from the theoretical density (predicted from those of the two constituents) and density measurements performed by hydrostatic weighting. The remaining porosity being generally less than 1.5%, it may be though that cracks and debonding do not affect significantly the overall porosity.

3.2.2. Comparison between experimental results and analytical predictions

The room temperature Young's modulus of model biphased samples has been determined using the ultrasonic waves propagation in "infinite medium mode" with contact transducers.[4] Experimental results are summarized in Table 2. For a given alumina volume fraction in iso CTE configuration (alumina/G2), the mean E values are always greater than those obtained in the two others cases.

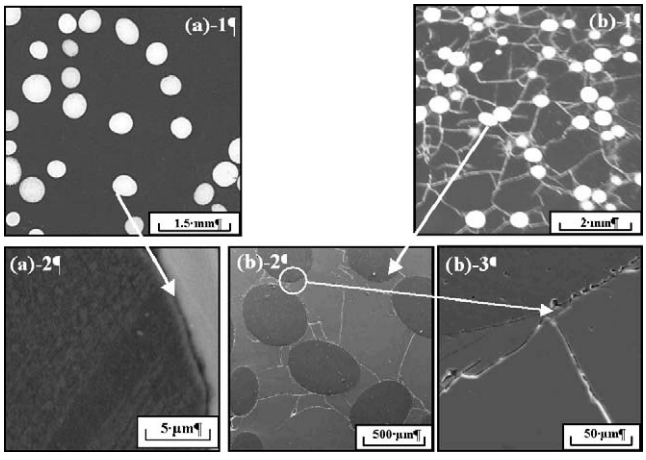

Fig. 2. Micrographs of 15 vol.%. model samples: (a) alumina/G1, (b) alumina/G3.

Among the various theoretical approaches developed to predict the overall elastic properties of biphased materials, the Voigt[5] and Reuss[6] bounds are widely used because of their simplicity. More accurate, the lower bound of Hashin and Shtrikman (E_v^-), which postulates a perfect bonding between the components, seems well suited to describe inclusional materials.[7] For spherical inclusions covered by a shell of softer matrix, the overall Young's modulus can be predict from the knowledge of the volume fractions (v_m, v_p) and those of shear and bulk moduli of each phase (G_m, G_p, K_m, K_p) only:

$$K_v^- = K_m + \frac{v_p}{[1/(K_p - K_m)] + [3v_m/(3K_m + 4G_m)]} \quad (1)$$

$$G_v^- = G_m + \frac{v_p}{[1/(G_p - G_m)] + [6(K_m + 2G_m)v_m/ 5G_m(3K_m + 4G_m)]} \quad (2)$$

E_v^- can be calculated using the following relationship:

$$E_v^- = \frac{9K_v^- G_v^-}{3K_v^- + G_v^-} \quad (3)$$

As shown in Fig. 3, experimental Young's modulus values for systems with adjusted interfaces are very close to the Hashin and Shtrikman's lower bound (HS^-). This result agrees with general investigations on such particulate reinforced materials.[8] For systems exhibiting CTE mismatch (alumina/G1 and alumina/G3), plots of experimental E values are lower than the HS^- prediction. This result denotes the impact of flaws, significantly greater for microcracked materials than for debonded ones.

Table 2
Young's modulus experimental values for alumina/glass materials

Alumina content (v_p)	$E_{experimental}$ (GPa)		
	Alumina/G1	Alumina/G2	Alumina/G3
15	73	93	30
30	92	115	33
45	98	139	49

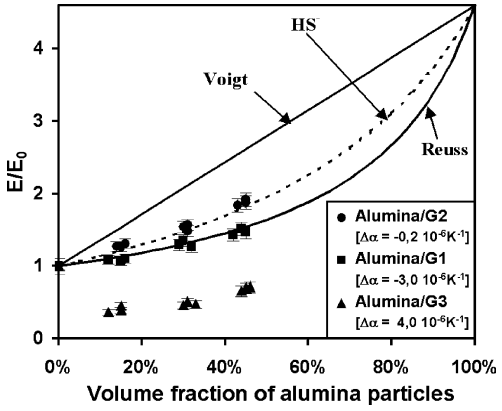

Fig. 3. Comparison between experimental Young's modulus and analytical predictions at room temperature.

3.3. Elastic properties versus temperature

3.3.1. Individual constituents

In a preliminary stage, the behaviour of glass matrices and inclusions are studied separately. The dispersed phase is constituted of 99.9% pure alumina beads but such near-spherical bodies are not suitable for direct high temperature thermoelastic properties measurement. So, E and α have been estimated using a previously sintered bar of similar alumina.

The Young's modulus was measured using the ultrasonic technique previously described and the linear thermal expansion $\Delta L/L_0$ by means of a horizontal dilatometer. The average thermal expansion coefficient [$\alpha_{CTE} = d(\Delta L/L_0)/dT$] was calculated between 50 and 450 °C for all constituents (Table 1) and the glass transition temperature T_g is obtained by intersecting the two linear parts of the $\Delta L/L_0$ versus temperature curve (slope change).

Measurement were performed above the glass softening point (T_s) with the same heating/cooling rate (5 °C min^{-1}) both for E and α estimation. However, the α variations during cooling are not shown because of the creep occurring beyond T_g.

As usually observed for most fine-grained ceramics, the results show a regular and slow reversible Young's modulus decrease (Fig. 4). As expected, matrices evolutions agree with this of alumina, except around T_g (drop on the curve). Indeed, softening induced by T_g appears at different temperatures and it varies slightly from one glass composition to another: the G1 and G2 Young's modulus decrease becomes faster than the G3 one.

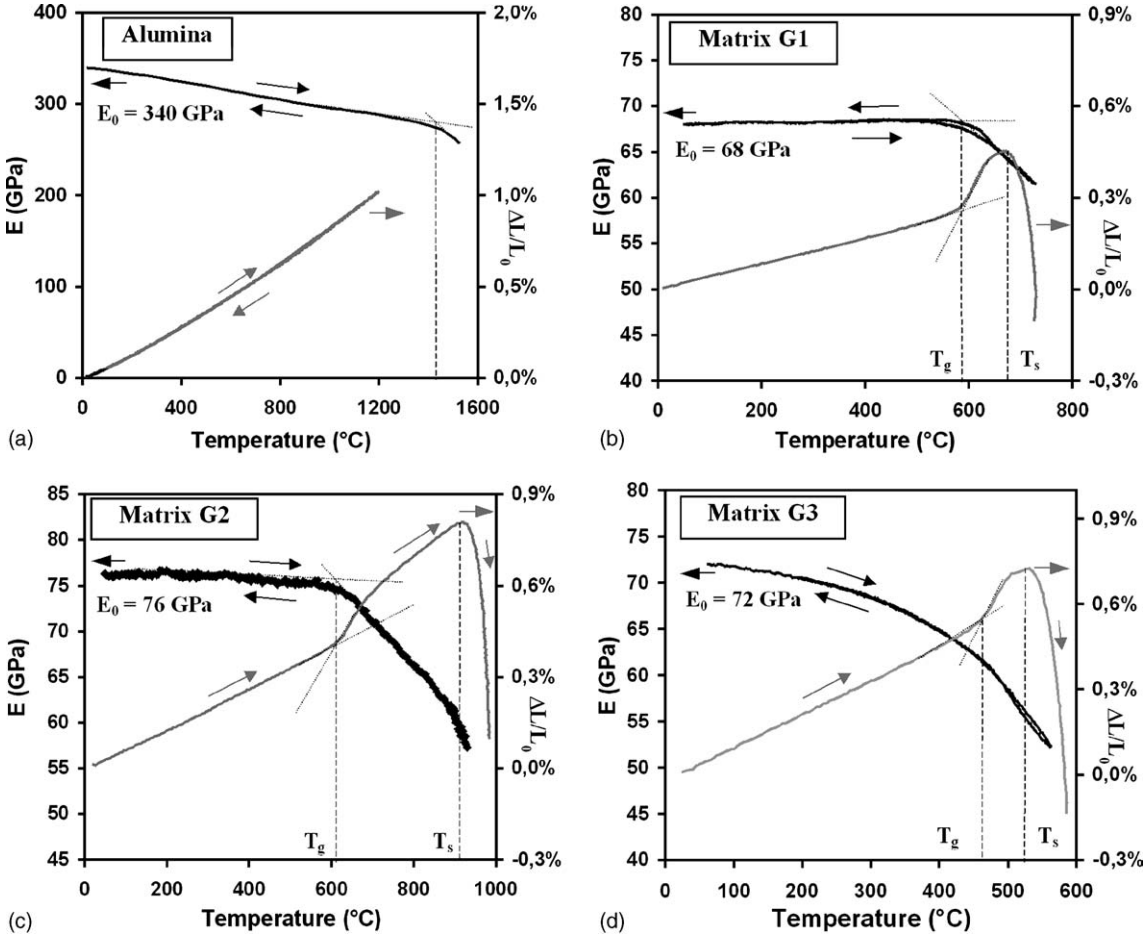

Fig. 4. Young's modulus vs. temperature and thermal expansion of the constituents: (a) alumina and (b–d) glass matrices.

3.3.2. Model materials with adjusted interfaces

Model samples prepared with G2 matrix show reversible evolution similar to that of the matrix (Fig. 5). The effective Young's modulus E_v^- corresponding to the lower Hashin and Shtrikman bound is also plotted in Fig. 5. Assuming that Poisson's ratios of each phase (υ_m and υ_p) are not temperature dependent,[9,10] $G_m(T)$ and $K_m(T)$ are calculated from the previous experimental $E_m(T)$ and $E_p(T)$ values thanks to the following relationships:

$$G = \frac{E}{2(1+\upsilon)} \quad (4)$$

$$K = \frac{E}{3(1+2\upsilon)} \quad (5)$$

E_v^- is obtained by combination of Eqs. (3)–(5). For $\Delta\alpha \neq 0$, a good correlation with experimental results is observed on the whole temperature range.

3.3.3. Model materials with interfacial debonding

For these materials the thermal CTE mismatch between matrix and alumina particles is $-3.0 \times 10^{-6}\,K^{-1}$. As already observed on Fig. 3, experimental initial modulus E_0 at 20 °C is significantly lower than E_v^- for the three volume fractions (Fig. 6). This result indicates the expected debonding state of the particles into the matrix. When heating, an increase of E is noticeable just after 300 °C. Then E increases slowly up to a dwell around 550 °C. This stage corresponds to the closure of interfacial debonding, probably incomplete at this temperature: because the glass softening mechanism is predominant up to 820 °C, the biphased materials exhibit the matrix behaviour.

During cooling, the experimental values join and follow the HS^- bound. This trend indicates a best interfacial contact of particles as previously seen. The Young's modulus level of free interfacial gap material is recovered. Between about 300 °C and room temperature, the curves move away from the predictive model: the mechanical adhesion of interfaces decreases and decohesions open again. Henderson et al.[11] have shown similar results from stress-train behaviour of commercial refractory materials exhibiting damaged interfaces.

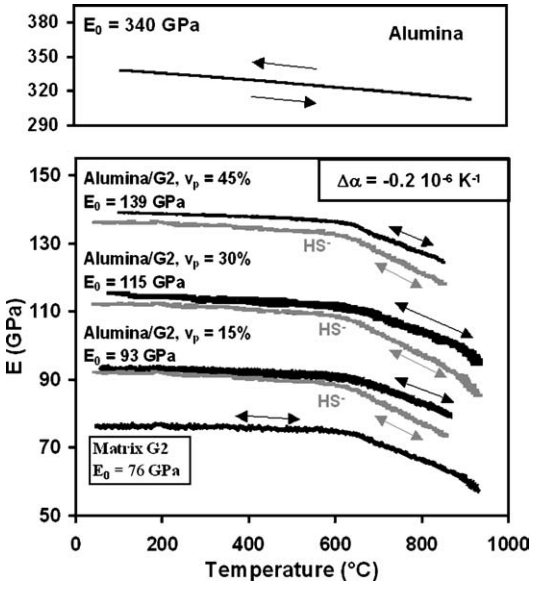

Fig. 5. Young's modulus vs. temperature: alumina/G2 samples [$\Delta\alpha = -0.2 \times 10^{-6}\,K^{-1}$].

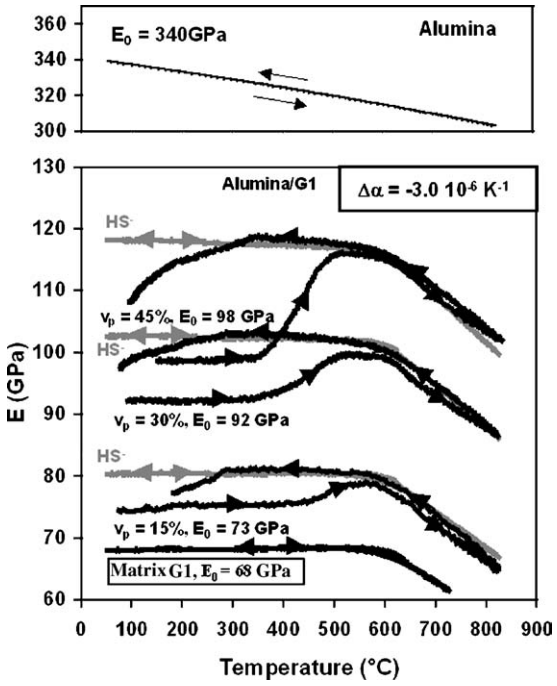

Fig. 6. Young's modulus vs. temperature: alumina/G1 samples [$\Delta\alpha = -3.0 \times 10^{-6}\,K^{-1}$].

The hysteresis degree increases with the volume fraction of alumina balls. The narrow dependence of the overall decohesive surface area on the number of inclusions may explain such an experimental result.

3.3.4. Model materials with matrix microcracking

For specimens presenting microcraking damages ($\Delta\alpha = 4.0 \times 10^{-6}\,K^{-1}$), the room temperature Young's modulus is significantly lower than the predicted HS^- bound (Fig. 7). E is quite constant between 20 °C and T_g, then it exhibits a sudden increase whereas matrix becomes viscous: the dwell and the following small decrease of E prove the competition between the flaws resorption process (increase) and the matrix softening (decrease). For the 45 vol.%. sample, a new increase of Young's modulus after 580 °C probably means that cracks closure occurs in two stages. During cooling, the good correlation with the HS^- bound from 660 to 200 °C suggests that the microcrack healing stage is nearly complete if the sample has been previously heated at a temperature above the softening point. Finally, the tensile stresses applied to the matrix become critical and a large microcracking of glass occurs, which leads to drastic change in Young's modulus versus temperature

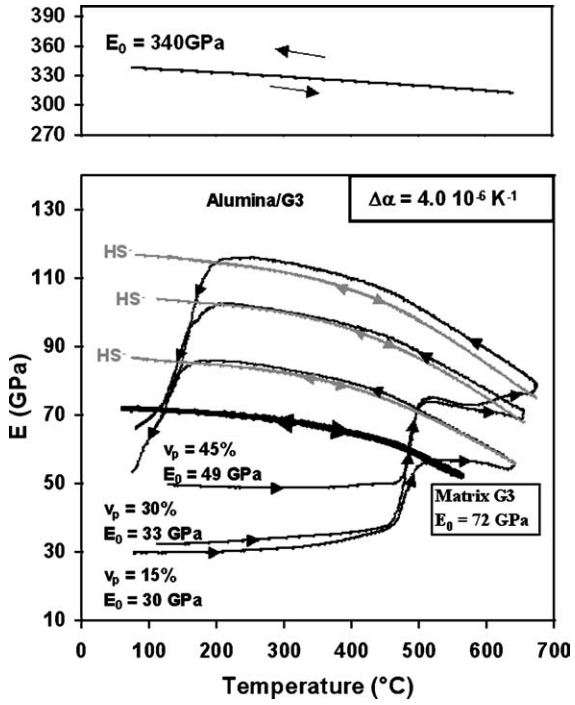

Fig. 7. Young's modulus vs. temperature: alumina/G3 samples [$\Delta\alpha = 4.0 \times 10^{-6}\,K^{-1}$].

curves. The final E value indicates that the initial degree of microcracking is not fully recovered.

4. Discussion

For a given volume fraction of alumina balls, E is more sensitive to matrix cracks than to interfacial gaps. The development of such flaws can be explained by the thermal stresses level during cooling.[12] When temperature varies, the hydrostatic pressure at the interface between the inclusion and the matrix can be expressed as:

$$p = \frac{(\alpha_m - \alpha_p)\Delta T}{[(1+\nu_m)/2E_m] + [(1-2\nu_p)/E_p]} \quad (6)$$

m and p subscripts denote the matrix and the particles, respectively. α stands for the thermal expansion coefficient, E for Young's modulus, ν for Poisson's ratio. ΔT represents the temperature cooling range over which the interfacial zone is free of stress.

Radial (σ_{rr}) and circumferential ($\sigma_{\theta\theta}$) stresses, respectively, perpendicular and parallel to the interface, can be calculated according to:

$$\sigma_{rr} = -p \quad (7)$$

$$\sigma_{\theta\theta} = \frac{p}{2} \quad (8)$$

For negative $\Delta\alpha$ values, during cooling the matrix is subjected to radial tensile stresses whose magnitude can give rise to a debonding of the interface, this latter being postulated cohesive above T_g. The resulting interfacial gap (Fig. 8) can increase with the $\Delta\alpha$ range. On the contrary, positive $\Delta\alpha$ values subject the particle to a compressive stress state. So, the matrix endures radial compressive stresses and circumferential tensile stresses. The matrix plasticity being not able to accommodate the relative displacements, the arising of these circumferential tensile stresses leads to radial microcracking of the glass.

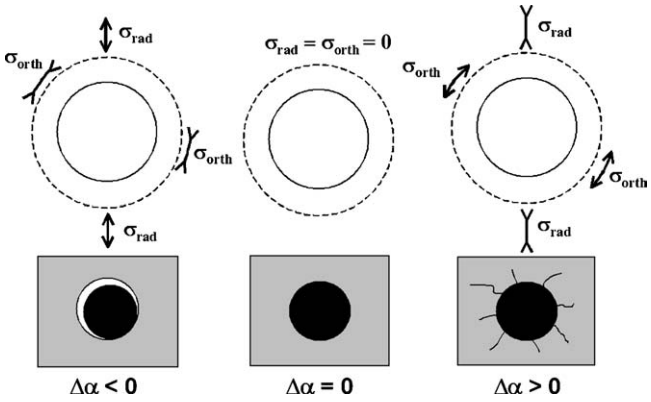

Fig. 8. Schematic representation of internal thermal stresses occurring during the cooling stage of a spherical inclusion embedded in an infinite isotropic phase.

It may be thought that cracks propagation along interfaces can be also responsible for particles debondings in systems for which $\Delta\alpha > 0$.

So, whatever the case is ($\Delta\alpha < 0$ or $\Delta\alpha > 0$), the defects induced by thermal stresses lead to Young's modulus decrease. Therefore, once such a decrease is observed during cooling, it is not possible to identify the type of defect responsible for this behaviour.

Finally, quite CTE equality gives stress free interfaces, the inclusion and the matrix being subjected to the same strain state.

5. Conclusion

Industrial refractories are highly heterogeneous multiphased materials: the size of their constituents can range from submicronic particles for binding phase powders to several millimetres for the biggest aggregates. Because of CTE disagreements, temperature variations induce microstructural flaw variations. It has been shown that model materials (hot-pressed glass matrix containing spherical alumina inclusions) with various CTE mismatches can exhibit similar Young's modulus temperature effects than industrial refractories.

The most significant results of this work are as follows:

- Young's modulus is highly sensitive to microstructural variations of multiphased materials;
- hysteresis cycles curves observed for industrial refractories are often due to interfacial debonding and matrix microcracking;

- Young's modulus versus temperature evolutions of the studied biphased model materials depend on the CTE disagreement between matrix and inclusions.

Many approximations have been assumed to carried out this study, chiefly dealing with the model materials composition, obviously far from this of usual refractories. On one hand, the binding phase is a glass matrix, well known to be bad temperature resistant and, on the other hand, two phases are considered only. Nevertheless, such biphased model materials appear as rather well suited to understand the behaviour of some actual refractories.

The analytical model of Hashin and Shtrikman exhibits good capabilities for materials containing inclusions with adjusted interfaces but is not suitable for damaged materials. Predicting models able to take into account the defects influence will become highly complicated. So, if the non-reversible behaviour occurring during the stages of heating/cooling must be taken into account, the approach by means of numerical simulation[13] seems a better way.

References

1. Huger, M., Fargeot, D. and Gault, C., High temperature measurement of ultrasonic wave velocity in refractory materials. *High Temp. High Pressure*, 2002, **34**, 193–201.
2. Vaudez, S., Huger, M. and Gault, C., Mechanical behaviour of Al_2O_3/C shaped refractories used in continuous casting. In *Proceedings of the 6th Conference of ECERS, Vol 60*, 1999, pp. 159–160.
3. Peruzzi, S., Vaudez, S., Huger, M., Gault, C., Glandus, J. C., Guillo, P. *et al.*, Thermomechanical modelling of alumina-graphite ladle shrouds used in continuous casting. In *Proceedings of UNITECR '99*, 1999, pp. 128–132.
4. Cutard, T., Fargeot, D., Gault, C. and Huger, M., Time delay and phase shift measurements for ultrasonic pulses using autocorrelation methods. *J. Appl. Phys.*, 1994, **75**, 1909–1913.
5. Voigt, W., *Lehrbuch der Kristallphysik*. Teubner, Berlin, 1910.
6. Reuss, A., Berechnung der Fliessgrenze von Mischkristallen auf Grund der Plastizitätsbedingung für Einkristalle. *Z. Angew. Math. u. Mech.*, 1929, **9**, 49–58.
7. Hashin, Z. and Shtrikman, S., A variational approach to the theory of the elastic behavior of multiphase materials. *J. Mech. Phys. Solids*, 1963, **11**, 127–140.
8. Ravichandran, K. S., Elastic properties of two-phase composites. *J. Am. Ceram. Soc.*, 1994, **77**(5), 1178–1184.
9. Sakaguchi, S., Murayama, N., Kodama, Y. and Wakai, F., The Poisson's ratio of engineering ceramics at elevated temperature. *J. Mater. Sci. Lett.*, 1991, **10**, 282–284.
10. Lemercier, H., *Verres du Système Y-Si-Al-O-N: Propriétés, Structure et Christallisation*. Ph.D. thesis, University of Limoges, France, 1995.
11. Henderson, R. J., Chandler, H. W. and Strawbridge, I., A model for non-linear mechanical behavior of refractories. *Br. Ceram. Trans.*, 1997, **96**(3), 85–91.
12. Selsing, S., Internal stresses in ceramics. *J. Am. Ceram. Soc.*, 1961, **44**(8), 419–426.
13. Tessier-Doyen, N., Huger, M. and Glandus, J. C., Etude Expérimentale et Numérique du Comportement Elastique de Matériaux Hétérogènes Modèles. In *Proceedings of Congress "Matériaux 2002"*, 2002, AF07042.